arXiv:1404.5880v2 [cond-mat.mtrl-sci] 1 Aug 2014

Anti-plane Shear Waves in Layered Composites: Band Structure and Anomalous Wave-refraction

Sia Nemat-Nasser

Department of Mechanical and Aerospace Engineering
University of California, San Diego
La Jolla, CA, 92093-0416 USA

Abstract

For oblique anti-plane shear waves in periodic layered elastic composites, it is shown that *negative energy refraction is accompanied by positive phase-velocity refraction* and *positive energy refraction is accompanied by negative phase-velocity refraction*, and that, this happens over a broad range of frequencies. The composite's unit cell may consist of any number of layers of any variable mass-density and elastic shear modulus (with large discontinuities).

Explicit series expressions for displacement, velocity, strain and stress components, and energy-flux fields are given, and group-velocity vector is calculated. The approach is based on a mixed variational principle where the displacement and stress components are viewed as independent fields subject to arbitrary variation. These fields are hence approximated independently, thereby ensuring the necessary continuity conditions. The resulting computational method yields the composite's frequency band structure and the associated mode shapes, in terms of the wave-vector components for any desired number of frequency bands. The calculations are direct and require no iteration, accurately and efficiently producing the entire band structure of the composite. This also allows for direct calculation of the components of the group-velocity, energy-flux, and phase-velocity vectors as functions of the frequency and wave-vector components, over an entire frequency band.

The general results are illustrated using a two-phase and a three-phase unit cell with piecewise constant properties. It is shown that the directions of the group-velocity and energy-flux vectors are essentially indistinguishable for this class of problems, and, more importantly that, on their second frequency pass-bands, *only the components of the phase and group velocities normal to the layers are antiparallel, while the components along the layers*

are parallel. Therefore, both the two-phase and the three-phase composites *display negative energy refraction with positive phase-velocity refraction* and *positive phase-velocity refraction with negative energy refraction*, depending on how the composite is interfaced with a homogeneous solid.

The presented method is applicable and effective also when some or all of the layers in a unit cell have spatially varying properties.

Keywords: Anti-plane shear waves, anomalous energy-flux and phase-velocity refraction, layered composites

---

1. Introduction

Elastic composites can have remarkable mechanical and acoustic properties that are not shared by their individual constituents. They have found widespread applications and hence have been extensively studied; see for example (Willis (1981b), Christensen (2012), Nemat-Nasser and Hori (1993, 1999), Maldovan and Thomas (2009), Banerjee (2011), Green (1991)). Here the focus is on harmonic waves in layered elastic composites, and their dynamic properties (Willis (1981a), Nayfeh (1995), Milton and Willis (2007), Willis (2013b)). In this context, efficient and accurate calculation of their band structure for Bloch-form harmonic waves is the necessary first step in estimating their overall response and effective dynamic constitutive properties (Nemat-Nasser and Srivastava (2011), Nemat-Nasser et al. (2011)). Various techniques have been used to study the dynamic responses of laminated composites; see Sigalas et al. (2005) for a review of recent contributions. This includes, for example, methods such as direct analytic solutions for layered composites (Rytov (1956), Mal (1988), Braga and Herrmann (1992)); transfer matrix (Thomson (1950), Gilbert and Backus (1966), Bahar (1972), Hosten and Castaings (1993), Rokhlin and Wang (2002)); plane-wave expansion (Nayfeh (1991)); displacement-based variational methods (Goffaux and Sánchez-Dehesa (2003), Goffaux et al. (2004)); and finite elements (Langlet et al. (1995), Åberg and Gudmundson (1997), Aboudi (1986)).

A general feature of layered composites is the presence of finite discontinuities in the properties (mass-density and stiffness) of their constituents. This renders the application of the usual Rayleigh quotient computationally ineffective (Kohn and Lee (1972), Nemat-Nasser (1973)).

To produce an effective tool that accounts for discontinuities as an integral part of the variational formulation, a mixed variational method has been developed and successfully used in the 1970's to calculate the band structure of one, two, and three-dimensional periodic elastic composites; (Nemat-Nasser (1972a), Nemat-Nasser (1972b), Nemat-Nasser et al. (1975), Minagawa and Nemat-Nasser (1976)). This mixed variational method yields very accurate results and the rate of convergence of the corresponding approximating series solution is greater than that of the Rayleigh quotient with displacement-based approximating functions (Babuška and Osborn (1978)). Since it is based on a variational principle, any set of approximating functions can be used for calculations, e.g., plane-waves Fourier series, as in the above cited papers, or finite elements (Minagawa et al. (1981)).

The method has been revived in recent years and applied to calculate the effective overall dynamic constitutive parameters of periodic composites for Bloch waves traveling normal to the layers (Nemat-Nasser et al. (2011)). The limits of the accuracy of the resulting estimates have been examined by considering the response of a layered composite interfaced with its homogenized half-space (Srivastava and Nemat-Nasser (2014); see also, Willis (2013a)).

When elastic waves are at an angle relative to an interface of a half-space layered composite, they generate a complex set of reflected and transmitted waves due to the inherent structure of the layered (or its homogenized) medium. It was recently suggested by Willis (2013b) that this complexity is avoided by considering oblique anti-plane shear waves. This then allows the study of a number of physically interesting phenomena, such as negative refraction, within a relatively simple mathematical framework. Willis (2013b) shows negative energy refraction when a layered composite is interfaced with a homogeneous solid on a plane normal to the layers. Here, we revisit this and in addition show that, unlike metamaterials, such negative refraction is accompanied by positive phase-velocity refraction.

The calculation of the band structure, mode shapes, group-velocity, and energy-flux vectors in terms of the wave-vector components for a wide range of frequencies, is a challenging task. Here this problem is addressed, successfully formulated, and solved using a mixed variational method to calculate *the entire band structure and the associated mode shapes* for oblique anti-plane shear waves in layered elastic composites. The composite may consist of periodically distributed unit cells of any number of layers of any desired properties that may vary in the direction normal to the layers. The results are then used to study the overall dynamic response of this class of composites. The problem is formulated for general unit cells and the results are illustrated using two-phase and three-phase unit cells. It is shown by direct calculation that the method easily produces any desired frequency band in terms of the wave-vector components and/or the angle that the wave vector makes with the direction normal to the layers. For illustration, numerical results for two- and three-phase unit cells are worked out in detail, where the material properties of each layer are uniform.

It is shown that composites with *two- and three-phase unit cells may display negative refraction*, which however is accompanied by *positive phase-velocity refraction*. Indeed, for this class of composites, it is shown that *only the components of the phase and group velocities normal to the layers are antiparallel while the corresponding components along the layers are parallel.*

This phenomenon is demonstrated by considering the refraction and reflection of plane waves when the composite is in contact with a homogeneous solid on a plane normal to the layers, as well as when the contact plane is parallel to the layers. In the first case, negative energy refraction with positive phase refraction may occur, and, in the second case, positive energy refraction with negative phase refraction may occur.

The calculations are direct and require no iteration, producing the entire band structure of the composites with unit cells of any number of layers of any constant or variable properties. This also yields explicit series-form expressions for all the field variables necessary to calculate the components of the group-velocity and the energy-flux vectors, from which the overall response of the composite can readily be extracted.

When the phase-velocity and energy-flux vectors are antiparallel, the resulting waves have been called *backward waves* or BW (Oliner and Tamir (1962), Lindell et al. (2001)). In general, backward waves and negative refraction occur when the wave-vector and the energy-flux vector are antiparallel. Here, for the layered composite, we show *negative energy refraction* with *positive phase refraction*, that is, we show that only one component of the phase velocity is antiparallel with its corresponding component of the energy-flux (or group velocity) vector while the other component of these vectors are parallel, leading to negative refraction with positive phase refraction. A similar phenomenon was first recognized to exist in photonic crystals by Gajic et al. (2005). In addition, we show here that *negative phase refraction* can occur with *positive energy refracttion*.

2. Statement of the Problem and Field Equations

Consider a layered composite and take the x_1-axis normal, and the x_2 and x_3 parallel to the layers. With a denoting the length of a typical unit cell, the mass-density $\hat{\rho}$ and the elastic shear moduli, $\hat{\mu}_{jk}$, $j,k = 1,2$, with $\hat{\mu}_{12} = \hat{\mu}_{21}$, have the periodicity of the composite, i.e.,

$$\hat{\rho}(x_1) = \hat{\rho}(x_1 + ma); \quad \hat{\mu}_{jk}(x_1) = \hat{\mu}_{jk}(x_1 + ma), \quad j,k = 1,2, \tag{1}$$

for any integer m.

For Bloch-form time-harmonic anti-plane shear waves of frequency ω and wave-vector components k_1 and k_2, the nonzero displacement component $\hat{u}_3(x_1, x_2, t)$ has the following structure:

$$\hat{u}_3 = u_3^p(x_1) e^{i(k_1 x_1 + k_2 x_2 - \omega t)}, \tag{2}$$

where $u_3^p(x_1)$ is periodic with the periodicity of the unit cell.

Set

$$\xi_1 = x_1/a, \quad \xi_2 = x_2/a, \quad Q_1 = k_1 a \quad Q_2 = k_2 a, \tag{3}$$

introduce the average parameters,

$$\bar{\rho} = \int_{-1/2}^{1/2} \hat{\rho}(a\xi) d\xi, \qquad \bar{\mu}_{11} = \int_{-1/2}^{1/2} \hat{\mu}_{11}(a\xi) d\xi, \tag{4}$$

and consider the following dimensionless quantities:

$$\begin{array}{lll} \mu_{jk}(\xi_1) = \hat{\mu}_{jk}(a\xi_1)/\bar{\mu}_{11}, & \rho(\xi_1) = \hat{\rho}(a\xi_1)/\bar{\rho}, & \nu^2 = a^2\omega^2\bar{\rho}/\bar{\mu}_{11}, \\ w^p(\xi_1) = u_3^p(a\xi_1)\sqrt{\bar{\mu}_{11}}, & \tau_1 = \sigma_{13}/\sqrt{\bar{\mu}_{11}}, & \tau_2 = \sigma_{23}/\sqrt{\bar{\mu}_{11}}, \end{array} \tag{5}$$

where ν is the dimensionless frequency. Here the displacement, u_3^p, and the nonzero (shear) stresses, $\sigma_{13} = \sigma_{31}$ and $\sigma_{23} = \sigma_{32}$, are rendered nondimensional and denoted by w and τ_j, $j = 1, 2$, respectively. In what follows, the corresponding (engineering) strains, $2\epsilon_{13} = 2\epsilon_{31}$ and $2\epsilon_{23} = 2\epsilon_{32}$, will be denoted by γ_1 and γ_2, respectively. The (normalized) field equations then become,

$$\tau_{1,1} + \tau_{2,2} + \nu^2\rho w = 0; \quad \tau_j = \mu_{jk}\gamma_k \quad (k \ summed), \tag{6}$$

$$\gamma_1 = w_{,1} \quad \gamma_2 = iQ_2 w, \quad w = w^p e^{iQ_1\xi_1}. \tag{7}$$

In view of equations (6, 7) and (2), the shear stress τ_2 can be expressed in terms of τ_1 and w, as follows:

$$\tau_2 = \frac{\mu_{12}}{\mu_{11}}\tau_1 + \frac{iQ_2}{D_{22}}w, \tag{8}$$

where D_{22} is the corresponding component of the normalized elastic compliance matrix defined by,

$$\begin{pmatrix} D_{11} & D_{12} \\ D_{21} & D_{22} \end{pmatrix} = \frac{1}{\Delta}\begin{pmatrix} \mu_{22} & -\mu_{12} \\ -\mu_{21} & \mu_{11} \end{pmatrix}, \quad \Delta = \mu_{11}\mu_{22} - \mu_{12}^2.$$

Hence,

$$\tau_{2,2} = iQ_2\tau_2 = iQ_2\frac{\mu_{12}}{\mu_{11}}\tau_1 - \frac{{Q_2}^2}{D_{22}}w. \tag{9}$$

3. Variational Formulation

Consider now the following functional:

$$I =< \tau_j, w_{,j} > + < w_{,j}, \tau_j > - < D_{jk}\tau_k, \tau_j > -\nu^2 < \rho w, w >, \tag{10}$$

where $< gu, v >= \int_{-1/2}^{1/2} guv^* d\xi$ for a real-valued function $g(\xi)$ and complex-valued functions $u(\xi)$ and $v(\xi)$, with star denoting complex conjugate. In (10) w and τ_j are viewed as independent fields subject to arbitrary variations. It is easy to show (Nemat-Nasser et al. (1975)) that equations (6) are the Euler equations that render the functional I stationary. It is however, expedient to use (8) in (10) and consider τ_1 and w as the only independent fields subject to variations, especially since the periodicity in layered composites is only in one direction. Hence consider the functional,

$$\begin{aligned} I_1 =< \tau_1, w_{,1} > + < w_{,1}, \tau_1 > -iQ_2 < \frac{\mu_{12}}{\mu_{11}}\tau_1, w > +iQ_2 < \frac{\mu_{12}}{\mu_{11}}w, \tau_1 > \\ +Q_2^2 < \frac{1}{D_{22}}w, w > - < \frac{1}{\mu_{11}}\tau_1, \tau_1 > -\nu^2 < \rho w, w > . \end{aligned} \tag{11}$$

The first variation of I_1 with respect to w^* and τ_1^* yields, respectively,

$$\tau_{1,1} + [iQ_2\frac{\mu_{12}}{\mu_{11}}\tau_1 - \frac{Q_2^2}{D_{22}}w] + \nu^2\rho w = 0 \qquad \tau_1 = \mu_{11}w_{,1} + iQ_2\mu_{12}w, \tag{12}$$

which also follow from (6, 7) and (8).

To find an approximate solution of the field equations (12) subject to the Bloch periodicity condition (2), consider the following estimates:

$$w = \sum_{\alpha=-M}^{+M} W^{(\alpha)} e^{i(Q_1+2\pi\alpha)\xi_1}, \quad \tau_1 = \sum_{\alpha=-M}^{+M} T^{(\alpha)} e^{i(Q_1+2\pi\alpha)\xi_1}, \tag{13}$$

which automatically ensure the Bloch and continuity conditions.

Substitution into (11) now yields,

$$\begin{aligned} I_1 = \sum_{\alpha,\beta=-M}^{+M} \{ & T^{(\alpha)}[-i(Q_1+2\pi\alpha)]\delta_{\alpha\beta}W^{(\beta)*} + W^{(\alpha)}[+i(Q_1+2\pi\alpha)]\delta_{\alpha\beta}T^{(\beta)*} \\ & -iQ_2T^{(\alpha)}\Lambda^{(\alpha\beta)}[\mu_{12}/\mu_{11}]W^{(\beta)*} + iQ_2W^{(\alpha)}\Lambda^{(\alpha\beta)}[\mu_{12}/\mu_{11}]T^{(\beta)*} \\ & -T^{(\alpha)}\Lambda^{(\alpha\beta)}[1/\mu_{11}]T^{(\beta)*} + W^{(\alpha)}\Lambda^{(\alpha\beta)}[Q_2^2/D_{22} - \nu^2\rho]W^{(\beta)*}\}, \end{aligned} \tag{14}$$

where $\Lambda^{(\alpha\beta)}$ is a linear integral operator, defined by

$$\Lambda^{(\alpha\beta)}[f(\xi)] = \int_{-1/2}^{1/2} f(\xi) e^{i2\pi(\alpha-\beta)\xi} d\xi = \int_{-1/2}^{1/2} f(\xi) e^{-i2\pi(\beta-\alpha)\xi} d\xi = \Lambda^{(\beta\alpha)^*}[f(\xi)], \tag{15}$$

with $f(\xi)$ being a real-valued integrable function.

For an even function, $f(\xi) = f(-\xi)$ (symmetric unit cells),

$$\Lambda^{(\alpha\beta)}[f(\xi)] = 2\int_{0}^{1/2} f(\xi) cos(2\pi(\alpha-\beta)\xi) d\xi = \Lambda^{(\beta\alpha)}[f(\xi)]. \tag{16}$$

Furthermore, for a piecewise constant $f(\xi)$, e.g.,

$$f(\xi) = \begin{cases} f_1 & 0 < \xi < l_1/2 \\ f_2 & l_1/2 < \xi < l_2/2 \\ ... & \\ ... & \\ f_n & l_{n-1}/2 < \xi < 1/2 \end{cases} \tag{17}$$

with $l_n = 1$, one obtains,

$$\Lambda^{(\alpha\beta)}[f(\xi)] = \begin{cases} \sum_{a=1}^{n} \frac{f_a - f_{a+1}}{\pi(\alpha-\beta)} sin(\pi(\alpha-\beta)l_a) & \alpha \neq \beta \\ \sum_{a=1}^{n} (f_a - f_{a+1}) l_a = \bar{f} & \alpha = \beta, \quad f_{n+1} = 0. \end{cases} \tag{18}$$

Define an $N \times N$ matrix $\mathbf{\Lambda}[f(\xi)] = [\Lambda^{(\alpha\beta)}][f(\xi)]$, $\alpha, \beta = 0, \pm 1, ..., \pm M$, and $N = 2M + 1$, and note that, in view of linearity, for any two constants a_1 and a_2,

$$a_1 \mathbf{\Lambda}[f_1(\xi)] + a_2 \mathbf{\Lambda}[f_2(\xi)] = \mathbf{\Lambda}[a_1 f_1(\xi) + a_2 f_2(\xi)].$$

Also, let $\mathbf{H}$ be an $N \times N$ diagonal matrix with components $(Q_1 + 2\pi\alpha)\delta_{\alpha\beta}$. Then, (14) can be rewritten as,

$$I_1 = \begin{bmatrix} \mathbf{W} \\ \mathbf{T} \end{bmatrix}^T \begin{bmatrix} Q_2^2 \mathbf{\Lambda}[1/D_{22}] - \nu^2 \mathbf{\Lambda}[\rho] & i\{\mathbf{H} + Q_2 \mathbf{\Lambda}[\mu_{12}/\mu_{11}]\} \\ -i\{\mathbf{H} + Q_2 \mathbf{\Lambda}[\mu_{12}/\mu_{11}]\} & -\mathbf{\Lambda}[1/\mu_{11}] \end{bmatrix} \begin{bmatrix} \mathbf{W}^* \\ \mathbf{T}^* \end{bmatrix}. \tag{19}$$

For symmetric unit cells, I_1 may be written as,

$$I_{1s} = \begin{bmatrix} \mathbf{W}^* \\ \mathbf{T}^* \end{bmatrix}^T \begin{bmatrix} Q_2^2 \mathbf{\Lambda}[1/D_{22}] - \nu^2 \mathbf{\Lambda}[\rho] & -i\{\mathbf{H} + Q_2 \mathbf{\Lambda}[\mu_{12}/\mu_{11}]\} \\ i\{\mathbf{H} + Q_2 \mathbf{\Lambda}[\mu_{12}/\mu_{11}]\} & -\mathbf{\Lambda}[1/\mu_{11}] \end{bmatrix} \begin{bmatrix} \mathbf{W} \\ \mathbf{T} \end{bmatrix}. \tag{20}$$

Furthermore, when $\mu_{12} = 0$, we obtain,

$$I_2 = \begin{bmatrix} \mathbf{W}^* \\ \mathbf{T}^* \end{bmatrix}^T \begin{bmatrix} Q_2^2\mathbf{\Lambda}[\mu_{22}] - \nu^2\mathbf{\Lambda}[\rho] & -i\mathbf{H} \\ i\mathbf{H} & -\mathbf{\Lambda}[1/\mu_{11}] \end{bmatrix} \begin{bmatrix} \mathbf{W} \\ \mathbf{T} \end{bmatrix}. \quad (21)$$

Note that, in view of equation (16), $\mathbf{\Lambda}[f(\xi)]$ in (19) and (21) is real-valued for symmetric unit cells. Furthermore, when a symmetric unit cell consists of layers of uniform elasticities and densities, equation (18) gives $\Lambda^{(\alpha\beta)}[f(\xi)]$ explicitly.

Now, minimization of I_2 (or I_1 for $\mu_{12} \neq 0$) with respect to the unknown coefficients $W^{(\alpha)}$ and $T^{(\alpha)}$, results in an eigenvalue problem which yields the band structure of the composite for anti-plane Bloch-form shear waves,

$$\left[(\mathbf{I} + Q_2^2\mathbf{A}\mathbf{\Lambda}[\mu_{22}]) - \nu^2\mathbf{A}\mathbf{\Lambda}[\rho]\right]\mathbf{W} = \mathbf{0}, \qquad \mathbf{A} = \mathbf{H}^{-1}\mathbf{\Lambda}[1/\mu_{11}]\mathbf{H}^{-1}, \quad (22)$$

where $\mathbf{I}$ is the identity matrix. For given values of Q_1 and Q_2, the eigenvalues, ν, of equation$(22)_1$ are obtained from

$$det\left|(\mathbf{I} + Q_2^2\mathbf{A}\mathbf{\Lambda}[\mu_{22}]) - \nu^2\mathbf{A}\mathbf{\Lambda}[\rho]\right| = 0, \quad (23)$$

and for each eigenvalue, the corresponding displacement field, $\mathbf{W}$, is given by $(22)_1$, and the stress field by

$$\mathbf{T} = i\{\mathbf{\Lambda}[1/\mu_{11}]\}^{-1}\mathbf{H}\mathbf{W}. \quad (24)$$

Note that $\mathbf{H}$ is a diagonal matrix whose components are linear in Q_1.

From (6, 7)), the x_2-component of the shear stress, τ_2, and the x_1-component of the shear strain, γ_1, are given by,

$$\tau_2 = iQ_2\mu_{22}(\xi_1)\sum_{\alpha=-M}^{+M} W^{(\alpha)}e^{i(Q_1+2\pi\alpha)\xi_1}, \quad \gamma_1 = D_{11}(\xi_1)\sum_{\alpha=-M}^{+M} T^{(\alpha)}e^{i(Q_1+2\pi\alpha)\xi_1}. \quad (25)$$

As can be seen, $\mathbf{W}$ is real-valued and $\mathbf{T}$ is purely imaginary. Both are implicit functions of Q_1 and Q_2.

The periodic parts of the displacement, velocity, and stresss-components are summarize here for subsequent application,

$$w^p(\xi_1) = \sum_{\alpha=-M}^{+M} W^{(\alpha)}e^{i2\pi\alpha\xi_1}, \quad \dot{w}^p(\xi_1) = -i\nu\sum_{\alpha=-M}^{+M} W^{(\alpha)}e^{i2\pi\alpha\xi_1}, \quad (26)$$

$$\tau_1^p(\xi_1) = \sum_{\alpha=-M}^{+M} T^{(\alpha)} e^{i2\pi\alpha\xi_1}, \quad \tau_2^p(\xi_1) = iQ_2 \sum_{\alpha=-M}^{+M} W^{(\alpha)} \mu_{22}(\xi_1) e^{i2\pi\alpha\xi_1}, \quad (27)$$

where for each frequency band J, associated with an eigenvalue ν_J, equations (22, 24) yield the corresponding coefficients, $W_J^{(\alpha)}$ and $T_J^{(\alpha)}$; the subscript J has been omitted in the above expressions. Once $W^{(\alpha)}$ and $T^{(\alpha)}$ are calculated for a desired eigenvalue, ν, the above expressions give the periodic part of the field variables.

4. Phase and Group Velocities, and Energy Flux

For a given (symmetric) unit cell that consists of a given number of layers of prescribed mass densities and stiffnesses, matrices $\mathbf{A}$ and $\mathbf{\Lambda}[f(\xi)]$ in (22) can be computed explicitly using (16). The expression in the right-hand side of (23) will then depend parametrically on the wave-vector components, Q_1 and Q_2. The resulting eigenfrequencies, ν, can thus be expressed as functions of Q_1 and Q_2. These eigenfrequencies form surfaces in the (Q_1, Q_2, ν)-space, referred to as Brillouin zones. The first zone corresponds to $-\pi \leq Q_1, Q_2 \leq \pi$. We focus on this zone and examine the dynamic properties of layered elastic composites on the first and second frequency bands.

On each frequency band, the phase and group velocities are given by,

$$v_{Jk}^p = \frac{\nu_J Q_k}{Q_1^2 + Q_2^2} \quad v_{Jk}^g = \frac{\partial \nu_J}{\partial Q_k}, \quad k = 1, 2; \quad (28)$$

here and below, $J = 1, 2, ...$ denotes the frequency band and $k = 1, 2$, the x_1- and the x_2-directions, respectively. The group velocity defines the direction of the energy flux; it is given by given by

$$\alpha_J = atan(\frac{v_{J2}^g}{v_{J1}^g}). \quad (29)$$

The x_1- and x_2-components of the energy-flux vector are given by

$$E_{Jk} = \frac{\nu_J}{2\pi} \int_0^{\frac{2\pi}{\nu_J}} < Re(\tau_{Jk}(\xi_1, \xi_2, t)) Re(\dot{w}_J^*(\xi_1, \xi_2, t)) > dt = -\frac{1}{2} < \tau_{Jk}^p \dot{w}_J^{p*} >, \quad (30)$$

which is real-valued, where $k = 1, 2$. Substitution from (26, 27) results in,

$$E_{J1} = -\frac{1}{2} i\nu_J \sum_{\alpha=-M}^{+M} T_J^{(\alpha)} W_J^{\alpha}, \quad E_{J2} = \frac{1}{2} \nu_J Q_2 \sum_{\alpha,\beta=-M}^{+M} W_J^{(\alpha)} W_J^{(\beta)} \Lambda^{(\alpha\beta)}[\mu_{22}]. \quad (31)$$

The direction, β_J, of the energy-flux vector is hence given by,

$$\beta_J = atan(\frac{E_{J2}}{E_{J1}}). \tag{32}$$

It is known (Brillouin (1948)) that the direction, α_J, is essentially the same as the direction β_J of the energy flux for nondissipative media. We shall illustrate this in what follows.

An Important Cautionary Note: For an oblique anti-plane shear wave in a periodic layered elastic composite, the angle of incidence $\theta = atan(\frac{Q_2}{Q_1})$ cannot be arbitrary, limiting the admissible values of Q_2 depending on the structure and composition of the corresponding unit cell, as well as on values of Q_1.

5. Illustrative Examples

5.1. Example 1: A Two-Phase Composite

We now examine the dynamic response of a *two-phase* composite where the corresponding unit cell consists of a very stiff and a relatively soft layer; see Figure 1. We show that, on the second frequency pass-band of such

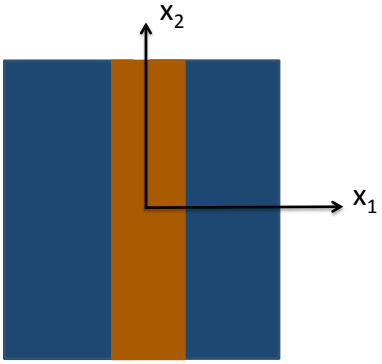

Figure 1: The unit cell of a two-phase composite.

composites, the group and phase velocities in the x_1-direction (normal to layers) are antiparallel (*backward wave*), whereas they are parallel in the x_2-direction (parallel to layers), signifying *the negative-energy refraction with positive phase refraction* characteristic of this class of elastic composites in

anti-plane shearing. In contrast, on the first frequency pass-band of the composite, the group and phase velocities are parallel, both in the x_1- and x_2-directions.

While the formulation and calculations are in terms of dimensionless quantities, in what follows the results are presented in terms of dimensional values for the symmetric unit cell shown in Figure 1. The dimensionless parameters and the results are calculated using the following specific material properties (typical for PMMA and steel):

1. $\mu_1 = 80 \times 10^9$ Pa; $\rho_1 = 8000$ kg/m^3; total thickness = 1.3mm
2. $\mu_2 = 3 \times 10^9$ Pa; $\rho_2 = 1180$ kg/m^3; total thickness = 3mm.

The unit cell is 4.3 mm thick. The resulting dimensionless parameters used in the calculations have the following values:

1. $\bar{\mu}_1 = 3.0442$; $\bar{\rho}_1 = 2.4677$; $\bar{h}_2 = 0.3023$
2. $\bar{\mu}_2 = 0.1142$; $\bar{\rho}_2 = 0.3640$; $\bar{h}_1 = 0.6977$.

The layers are isotropic, and subscripts $1, 2$ identify the properties (μ for shear modulus and ρ for density) of each layer within the unit cell. For example, μ_2 stands for $\mu_{11} = \mu_{22}$ of layer 2. The superimposed bar denotes the corresponding normalized value; see equations (4, 5). To obtain the frequency in kHz, and the group velocity, v^g_{Jk}, in m/s, multiply ν by 105, and v^g_{Jk} by 2847, respectively.

5.1.1. Frequency Band Structure

Now examine the variation of the frequency as a function of the wave-vector components, Q_1 and Q_2. For each pair of Q_1 and Q_2, the direction of the wave vector is obtained from $\theta = atan(Q_2/Q_1)$, the direction of the group-velocity vector from $\alpha_J = atan(v^g_{J2}/v^g_{J1})$ (which is shown below to be the same as that of the energy-flux vector, $\beta_J = atan(E_{J2}/E_{J1})$), and the direction of the phase-velocity from $\phi_J = atan(v^p_{J2}/v^p_{J1}) = \theta$, respectively.

Figure 2 shows the frequency (in kHz) as a function of Q_1 for indicated values of Q_2, and Figures 3(a, b) show the constant-frequency contours together with the direction of energy flow (superimposed arrows) as functions of Q_1 and Q_2, for the first two frequency pass-bands . As is seen, for suitably small values of Q_2 these contours are ellipses on the first pass-band whereas they are hyperbolae on the second pass-band. On the first frequency pass-band, the corresponding components of the energy-flux and the phase-velocity vectors are parallel, but not on the second frequency pass-band. In this later

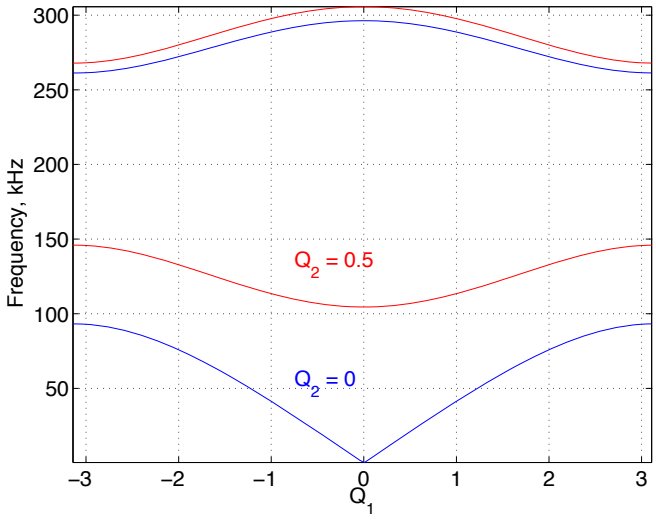

Figure 2: Frequency (in kHz) as function of Q_1 for indicated values of Q_2; two-phase composite.

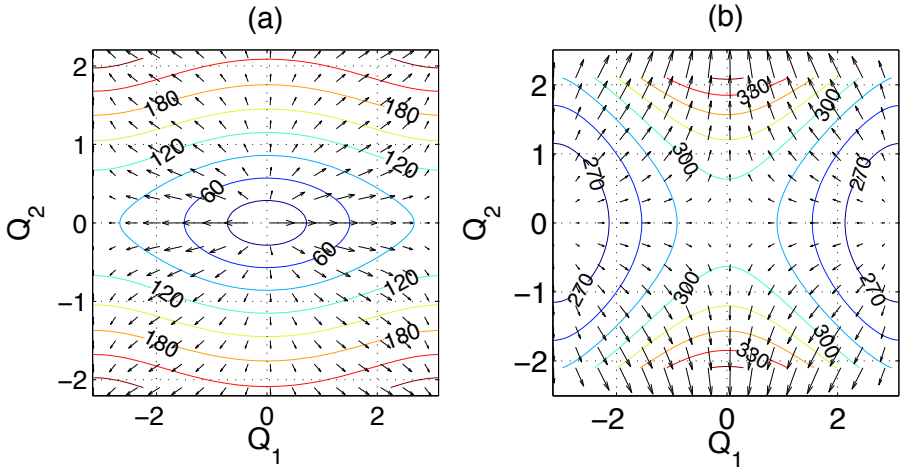

Figure 3: Contours of constant frequency (in kHz) and group-velocity vectors for: (a) first pass band, and (b) second pass band; two-phase composite; (for clarity, in graph (a) the x_2-component of the group velocity is reduced by a factor of 5).

case, the energy flux in the x_1-direction is antiparallel with the corresponding component of the phase-velocity, while in the x_2-direction these components are parallel. Hence the composite may or may not display *negative refraction*, depending on the direction of the incident wave, as shown in Figures 3(b). Here in addition, *negative energy refraction is accompanied by positive phase refraction* and *positive energy refraction is accompanied by negative phase refraction*; see subsection 5.2 for illustration. In terms of the group and phase velocities, in Figure 3(a), $v_1^g v_1^p > 0$ and $v_2^g v_2^p > 0$, whereas in Figure 3(b), $v_1^g v_1^p < 0$ but $v_2^g v_2^p > 0$.

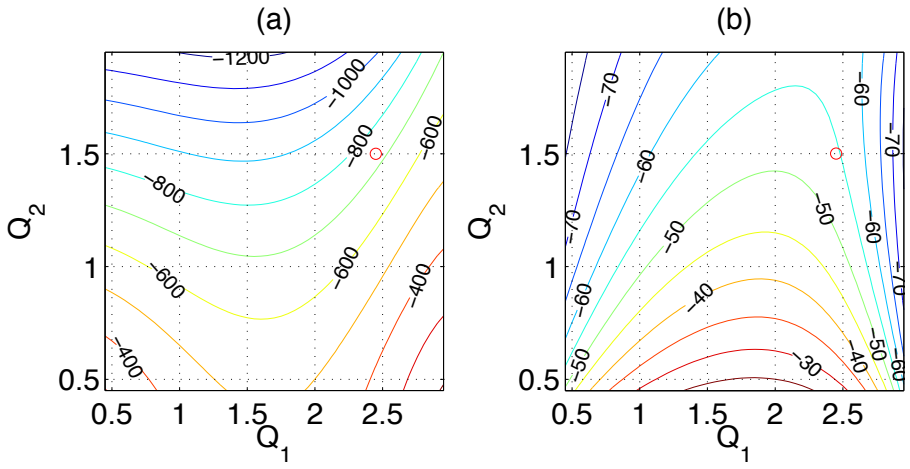

Figure 4: (a) Contours of constant group velocity (in m/s), and (b) contours of constant (energy) refraction angle; for second pass-band of a two-phase composite (negative sign signifies a negative angle with the x_1-axis). The red circles correspond to values for Example 5.2.

Focusing on the second frequency pass-band, we have presented in Figure 4(a) contours of constant group velocity (in m/s) and in Figure (4b) those of constant (energy-flux) refraction angle. As pointed out above, the group-velocity vectors are oriented in the direction of the energy flow. For positive wave-vector components, they have negative components in the x_1-direction but positive components in the x_2-direction; this is signified by negative signs in Figures 4(a, b).

As is mentioned before, the group velocity-vector defines the direction of energy flux. Figures (5a, b) show the refraction angles, (α_1 and β_1) and (α_2 and β_2), as functions of the frequency for $\theta = atan(\frac{Q_2}{Q_1}) = 10, 30^o$. The

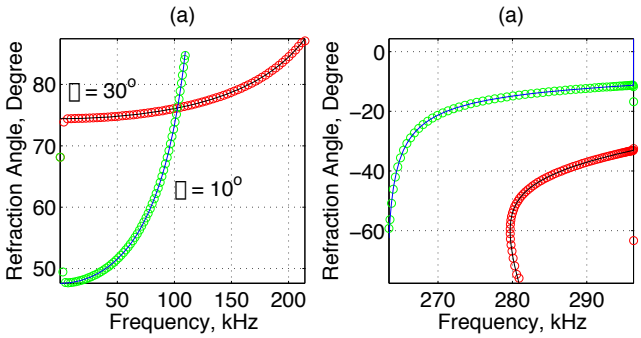

Figure 5: Refraction angle for indicated incident angles as functions of frequency; solid (black: 30^o; blue: 10^o) curves are energy-flux and open (red: 30^o; green: 10^o) circles are for group-velocity direction; (a) first frequency pass-band, and (b) second frequency pass-band.

solid curves correspond to the energy-flux and the open circles to the group-velocity directions. The figures show that the orientations of the group-velocity and energy-flux vectors are essentially indistinguishable.

5.2. Example 2: Negative Refraction with Positive Phase Velocity and Positive Refraction with Negative Phase Velocity

Examination of Figure 3 readily reveals that the layered composite can display negative refraction or negative phase-velocity refraction depending on how it is interfaced with a homogeneous solid. Figures 6(a,b) suggest two possible ways. In Figure 6(a), the layered composite occupies the half-space $x_2 > 0$ while a homogeneous solid (say, aluminum) is occupying the half-space $x_2 < 0$, whereas in Figure 6(b) the interface of the layered medium and aluminum is along the x_2-axis on the $x_1 = 0$-axis. In each case, a plane harmonic anti-plane shear wave of wave-vector $\mathbf{k}^{in}$ is incident from the homogeneous solid toward the interface at an incident angle θ_0, where $\theta = 10^o$ in Figure 3(a) and $\theta = 20^o$ in Figure 6(b). In the first case, negative refraction is accompanied by positive phase refraction, and in the second case this is reversed, namely positive refraction is accompanied by negative phase refraction.

Let C_0 be the shear-wave velocity in the homogeneous solid. Consider

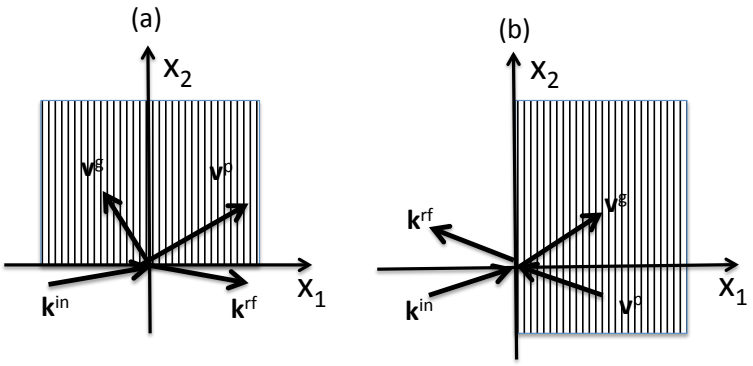

Figure 6: Plane harmonic wave of wave vector $\mathbf{k}^{in}$ is incident from (a) $x_2 < 0$ and (b) $x_1 < 0$ homogeneous half-space toward a periodic half-space; $\mathbf{k}^{rf}$ and $\mathbf{k}^{tr}$ are the reflected and transmitted wave vectors; $\mathbf{v}^g$ and $\mathbf{v}^p$ are the corresponding group and phase velocities.

Figure 6(a) and note that,

$$Q_1 = Q_1^{rf} = Q_1^{tr} = \frac{cos(\theta_0)}{\bar{C}_0}\nu, \quad Q_2 = -Q_2^{rf} = \frac{sin(\theta_0)}{\bar{C}_0}\nu, \quad \bar{C}_0 = C_0\sqrt{(\bar{\rho}/\bar{\mu}_{11})}, \tag{33}$$

where $\bar{C}_0$ is the dimensionless value of the shear-wave speed in the homogeneous $x_2 < 0$ half-space. For a given frequency, say ν_0, Q_1^{tr} is given by $(33)_1$ and Q_2^{tr} is calculated such that $\nu(Q_1^{tr}, Q_2^{tr}) = \nu_0$. For aluminum with a shear-wave speed of $C_0 = 3{,}040$ m/s and $\theta_0 = 10^o$, Figure (7) shows the variation of the frequency in kHz for $2.2 < Q_1 < 2.7$ and $1.2 < Q_2 < 1.8$. For a frequency $\cong$ 281.9 kHz ($\nu \cong 2.67$), we have $Q_1^{tr} = Q_1 \cong 2.47$, and $Q_2^{tr} = 1.50$. This gives a refraction angle of about -54.4^o and a group velocity of $\cong$ 733.5 m/s. These values are identifyed in Figures 4 and 7 by red circles.

Now consider Figure 6(b) and note that the phase angle $Q_2\xi_2 - \nu t$ on the $x_1 = 0$-axis must be continuous. Hence,

$$Q_2 = Q_2^{rf} = Q_2^{tr} = \frac{sin(\theta_0)}{\bar{C}_0}\nu, \quad Q_1 = -Q_1^{rf} = \frac{cos(\theta_0)}{\bar{C}_0}\nu. \tag{34}$$

For $\theta = 20^o$ and a frequency $\cong$ 280 kHz ($\nu \cong 2.65$), we have $Q_2^{tr} = Q_2 \cong 0.85$, and Q_1^{tr} = -1.50. This gives a refraction angle of about 37.3^o and a group velocity of $\cong$ 608.9 m/s.

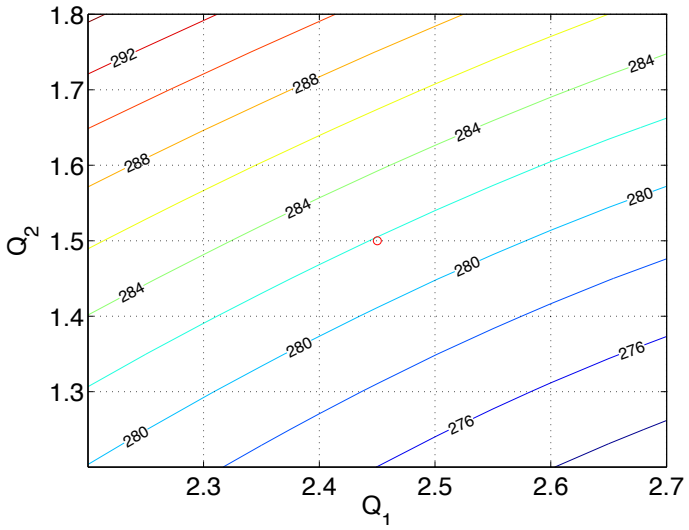

Figure 7: Contours of constant frequency (in kHz) for $2.4 < Q_1 < 2.6$ and $1.2 < Q_2 < 1.8$; second frequency pass-band.

5.3. Example 4: A Three-Phase Composite

Qualitatively, the three-phase layered composite has the same dynamic response as the two-phase composite considered above. As an illustration, consider a unit cell consisting of a central 1 mm thick layer of steel that is sandwiched by two layers of polyurea/phenolic-microballoon composite of 0.4 mm thickness each, and then by two layers of PMMA of 1.25 mm each, the total thickness of the unit cell being 4.3 mm, the same as the two-phase composite.

Figures (8a, b) display contours of constant frequency (in kHz) for the first (a) and the second (b) frequency pass-bands together with a representative number of group-velocity vectors; for clarity, the x_2-components of these vectors are reduced by a factor of 10. For suitably small values of Q_2, these contours are ellipses for the first pass-band, but they are hyperbolae for the second pass-band. Moreover, both of the components of the group-velocity vectors are parallel with the corresponding phase-velocity components on the first pass-band, but on the second frequency pass-band, only their x_2-components are parallel while their x_1-components are antiparallel with the corresponding components of the phase-velocity vectors. Hence, the refraction properties here are the same as those of the two-phase composites; see

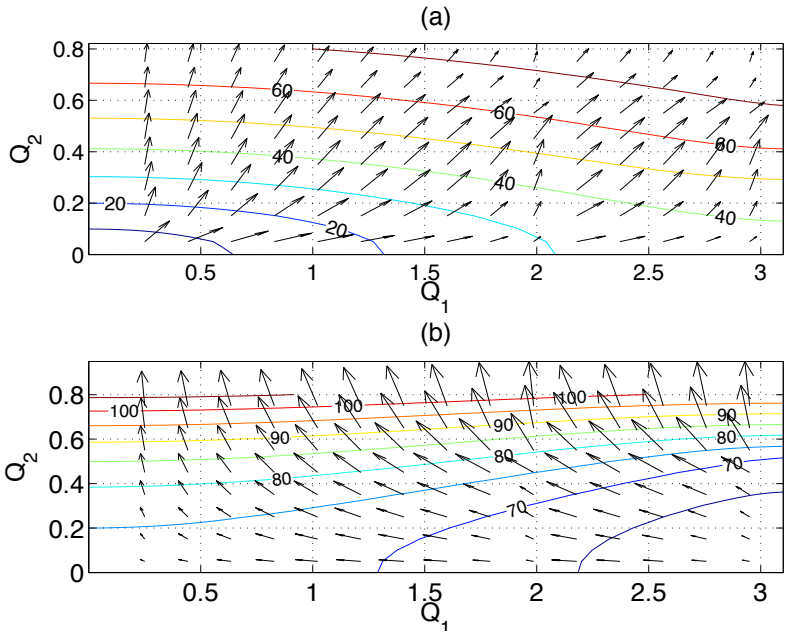

Figure 8: Contours of constant frequency (kHz): (a) first pass band, (b) second pass band, together with typical group-velocity vectors; the x_2-components of the group-velocity vectors are reduced by a factor of 10, and arrows are scaled for clarity; (three-phase unit cell).

Figures (6). Also, the direction of the group-velocity and and energy-flux vectors are the same.

Hence, in general for anti-plane shear waves, layered periodic composites display *negative refraction accompanied by positive phase-velocity refraction and positive refraction accompanied by negative phase-velocity refraction* depending how they are interfaced with a homogeneous material.

5.4. Discussion and Conclusions

Periodic elastic composites can be designed to have static and dynamic characteristics that are not shared by their constituent materials. Some of the dynamic characteristics and responses of layered periodic composites are explored in this work, using harmonic anti-plane shear waves. The considered composites lack periodicity in the direction parallel to the layers. This profoundly affects their dynamic response, leading to anomalous wave-refraction, namely, for this class of composites, negative refraction is accompanied by positive phase-velocity refraction, a phenomenon which was first recognized by Gajic et al. (2005). We have in addition shown that the composite can also display negative phase-velocity refraction accompanied by positive energy refraction, a phenomenon which does not seem to have been recognized before.

In the present work, a general variational approach is developed that produces the entire band structure of the composite for unit cells of any number of layers with any arbitrary properties. Explicit expressions are developed for the band structure, group-velocity and energy-flux vectors. The general results are illustrated using a two-phase and a three-phase unit cell with piecewise constant properties. The presented method is applicable and effective also when some or all of the layers in a unit cell have spatially varying properties.

Acknowledgments: This research has been conducted at the Center of Excellence for Advanced Materials (CEAM) at the University of California, San Diego, under DARPA AFOSR Grants FA9550-09-1-0709 and RDECOM W91CRB-10-1-0006 to the University of California, San Diego.

6. References

References

Åberg, M., Gudmundson, P., 1997. The usage of standard finite element codes for computation of dispersion relations in materials with periodic

microstructure. The Journal of the Acoustical Society of America 102, 2007.

Aboudi, J., 1986. Harmonic waves in composite materials. Wave motion 8 (4), 289–303.

Babuška, I., Osborn, J., 1978. Numerical treatment of eigenvalue problems for differential equations with discontinuous coefficients. Mathematics of Computation 32 (144), 991–1023.

Bahar, L. Y., 1972. Transfer matrix approach to layered systems. Journal of the Engineering Mechanics Division 98 (5), 1159–1172.

Banerjee, B., 2011. An Introduction to Metamaterials and Waves in Composites. CRC Press.

Braga, A. M., Herrmann, G., 1992. Floquet waves in anisotropic periodically layered composites. The Journal of the Acoustical Society of America 91, 1211.

Brillouin, L., 1948. Wave guides for slow waves. Journal of Applied Physics 19 (11), 1023–1041.

Christensen, R. M., 2012. Mechanics of composite materials. DoverPublications. com.

Gajic, R., Meisels, R., Kuchar, F., Hingerl, K., 2005. Refraction and rightness in photonic crystals. Optics express 13 (21), 8596–8605.

Gilbert, F., Backus, G. E., 1966. Propagator matrices in elastic wave and vibration problems. Geophysics 31 (2), 326–332.

Goffaux, C., Sánchez-Dehesa, J., 2003. Two-dimensional phononic crystals studied using a variational method: Application to lattices of locally resonant materials. Physical Review B 67 (14), 144301.

Goffaux, C., Sánchez-Dehesa, J., Lambin, P., 2004. Comparison of the sound attenuation efficiency of locally resonant materials and elastic band-gap structures. Physical Review B 70 (18), 184302.

Green, W. A., 1991. Reflection and transmission phenomena for transient stress waves in fiber composite laminates. In: Review of Progress in Quantitative Nondestructive Evaluation. Springer, pp. 1407–1414.

Hosten, B., Castaings, M., 1993. Transfer matrix of multilayered absorbing and anisotropic media. measurements and simulations of ultrasonic wave propagation through composite materials. The Journal of the Acoustical Society of America 94, 1488.

Kohn, W Krumhansl, J. A., Lee, E. H., 1972. Variational methods for dispersion relations and elastic properties of composite materials. Journal of Applied Mechanics 39 (2), 327–336.

Langlet, P., Hladky-Hennion, A.-C., Decarpigny, J.-N., 1995. Analysis of the propagation of plane acoustic waves in passive periodic materials using the finite element method. The Journal of the Acoustical Society of America 98, 2792.

Lindell, I. V., Tretyakov, S., Nikoskinen, K., Ilvonen, S., 2001. Bw media-media with negative parameters, capable of supporting backward waves. Microwave and Optical Technology Letters 31 (2), 129–133.

Mal, A., 1988. Wave propagation in layered composite laminates under periodic surface loads. Wave Motion 10 (3), 257–266.

Maldovan, M., Thomas, E. L., 2009. Periodic materials and interference lithography for photonics, phononics and mechanics. Wiley. com.

Milton, G. W., Willis, J. R., 2007. On modifications of newton's second law and linear continuum elastodynamics. Proceedings of the Royal Society A: Mathematical, Physical and Engineering Science 463 (2079), 855–880.

Minagawa, S., Nemat-Nasser, S., 1976. Harmonic waves in three-dimensional elastic composites. International Journal of Solids and Structures 12 (11), 769–777.

Minagawa, S., Nemat-Nasser, S., Yamada, M., 1981. Finite element analysis of harmonic waves in layered and fibre-reinforced composites. International Journal for Numerical Methods in Engineering 17 (9), 1335–1353.

Nayfeh, A. H., 1991. The general problem of elastic wave propagation in multilayered anisotropic media. The Journal of the Acoustical Society of America 89, 1521.

Nayfeh, A. H., 1995. Wave propagation in layered anisotropic media: With application to composites. Access Online via Elsevier.

Nemat-Nasser, S., 1972a. General variational methods for waves in elastic composites. Journal of Elasticity 2 (2), 73–90.

Nemat-Nasser, S., 1972b. Harmonic waves in layered composites. Journal of Applied Mechanics 39, 850.

Nemat-Nasser, S., 1973. Discussion: Variational methods for dispersion relations and elastic properties of composite materials. Journal of Applied Mechanics 40 (1), 327–336.

Nemat-Nasser, S., Fu, F., Minagawa, S., 1975. Harmonic waves in one-, two- and three-dimensional composites: bounds for eigenfrequencies. International Journal of Solids and Structures 11 (5), 617–642.

Nemat-Nasser, S., Hori, M., 1993, 1999. Micromechanics: overall properties of heterogeneous materials. Vol. 2. Elsevier Amsterdam.

Nemat-Nasser, S., Srivastava, A., 2011. Overall dynamic constitutive relations of layered elastic composites. Journal of the Mechanics and Physics of Solids 59 (10), 1953–1965.

Nemat-Nasser, S., Willis, J. R., Srivastava, A., Amirkhizi, A. V., 2011. Homogenization of periodic elastic composites and locally resonant sonic materials. Physical Review B 83 (10), 104103.

Oliner, A., Tamir, T., 1962. Backward waves on isotropic plasma slabs. Journal of Applied Physics 33 (1), 231–233.

Rokhlin, S., Wang, L., 2002. Stable recursive algorithm for elastic wave propagation in layered anisotropic media: Stiffness matrix method. The Journal of the Acoustical Society of America 112, 822.

Rytov, S., 1956. Acoustical properties of a thinly laminated medium. Sov. Phys. Acoust 2, 68–80.

Sigalas, M., Kushwaha, M. S., Economou, E. N., Kafesaki, M., Psarobas, I. E., Steurer, W., 2005. Classical vibrational modes in phononic lattices: theory and experiment. Zeitschrift für Kristallographie 220 (9-10), 765–809.

Srivastava, A., Nemat-Nasser, S., 2014. On the limit and applicability of dynamic homogenization. Wave Motion.

Thomson, W. T., 1950. Transmission of elastic waves through a stratified solid medium. Journal of Applied Physics 21, 89.

Willis, J., 1981a. Variational and related methods for the overall properties of composites. Advances in applied mechanics 21, 1–78.

Willis, J., 1981b. Variational principles for dynamic problems for inhomogeneous elastic media. Wave Motion 3 (1), 1–11.

Willis, J., 2013a. Some thoughts on dynamic effective properties–a working document. arXiv preprint arXiv:1311.3875.

Willis, J., 2013b. A study of obliquely propagating longitudinal shear waves in a periodic laminate. arXiv preprint arXiv:1310.6561.